Magnetizations and magneto-transport properties of Ni-doped $PrFeO_3$ thin films

Feroz A. Mir[a)†], S. K. Sharma[b)], and Ravi Kumar[c)]

[a)] University Science Instrumentation Center, University of Kashmir, J & K, Srinagar-190006, India
[b)] Instituto de Fisica Gleb Wataghin, Universidade Estadual de Campinas (UNICAMP), Campinas, 13.083- 970 Sao Paulo, Brazil
[c)] CMSE, National Institute of Technology, Hamirpur (H.P)-177005, India

(Received 11 May 2013; revised manuscript received 10 August 2013; published online 10 February 2014)

The present study reports the magnetizations and magneto-transport properties of $PrFe_{1-x}Ni_xO_3$ thin films grown by pulsed laser ablation technique on $LaAlO_3$ substrates. From DC M/H plots of these films, weak ferromagnetism or ferrimagnetism behaviors are observed. With Ni substitution, reduction in saturation magnetization is also seen. With Ni doping, variations in saturation field (H_s), coercive field (H_c), Weiss temperature (θ), and effective magnetic moment (p_{eff}) are seen. A small change of magnetoresitance with application of higher field is observed. Various essential parameters like density of state (N_f) at Fermi level, Mott's characteristic temperature (T_0), and activation energy (E_a) in the presence of and in the absence of magnetic field are calculated. The present observed magnetic properties are related to the change of Fe–O bond length (causing an overlap between the oxygen p orbital and iron d orbital) and the deviation of the Fe–O–Fe angle from 180°. Reduction of magnetic domain after Ni doping is also explored to explain the present observed magnetic behavior of the system. The influence of doping on various transport properties in these thin films indicates a distortion in the lattice structure and single particle band width, owing to stress-induced reduction in unit cell volume.

Keywords: thin films, magnetization, ferromagnetism, ferrimagnetism, magneto-transport and distortion

PACS: 81.15.Fg, 73.50.Jt, 75.50.Bb, 81.15.Fg **DOI:** 10.1088/1674-1056/23/4/048101

1. Introduction

In the last few decades, ABO_3 (A = rare-earth-metal and B = transition-metal) oxide-based materials have been on the center stage of the condensed matter community due to their potential technological applications, as well as their richness of science.[1–7] The perovskites in the $RFeO_3$ (R = La through Lu) series have the distorted orthorhombic $GdFeO_3$-type structure (with space group = $Pbnm$).[8] The distortion of the Fe ion in the octahedron is small and is almost independent of R. However, the distortion of the R coordination polyhedral is large and enhanced with the reduction in ionic radius of R. As distortion increases, the 12 O atoms surrounding the R atom separate into two types, i.e., eight first-nearest and four second nearest O atoms. Such structural distortions affect the magnetic ordering and spin state transitions.[9] In the cubic perovskite, the octahedral ligand field produced by the O atoms surrounding each Fe atom splits the 10-fold degeneracy of d levels of Fe atom into 6-fold t_{2g} and 4-fold e_g levels. Fe^{3+} has d^5 configuration. The distribution of five 3d electrons into these energy levels depends on the strength of the ligand field ($10D_q$) and the spin pairing energy. $RFeO_3$ orthoferrites are magnetically ordered semiconductors reflecting localized 3d electrons in the high spin (HS) state. The x-ray photoelectron spectra of these compounds[10] also reveals these features. Magnetic ordering of HS Fe^{3+} cation in the octahedral B sites is essentially antiferromagnetic (AFM) with a weak (canted) ferromagnetic (FM) component[11] and results from the strong Fe (B-site)–Fe (B-site) coupling between corner-sharing FeO_6 octahedra. The magnetic disordering temperature (T_N = Neel temperature) for the orthoferrite $RFeO_3$ has been measured by Eibschutz *et al.*[12] through observing the collapse of the magnetic hyperfine sextet into a singlet in the ^{57}Fe Mossbauer spectrum with variation in temperature. The R–O bonds become more covalent as the Fe–O bonds become more ionic and the Fe–O–Fe super-exchange interaction decreases with the decrease in ionic radii of the lanthanide ions. Therefore, the Neel temperature (T_N) across this series is lowered.[13]

In these ABO_3 compounds, both A and B cations can be partially substituted, hence leading to the $A_{1-x}A^*_xB_{1-y}B^*_yO_{3\pm\lambda}$ general formula. The partial substitutions of A^* for A of different oxidation states lead to the formations of vacancies of the crystalline bonds and also to stabilizations of unusual oxidation states of the B cation.[14] However, B site partial substitution by a B^* site cation can promote the changes of both the redox ion and the active site, and thus further effects on the stability of the crystalline structure[15] even at high temperatures. By definition, the perovskite structure acts as a host structure that, according to the substituting cation, can exhibit different transport behaviors.

Recently, the semiconducting and FM behaviors were shown in bulk polycrystalline $PrFe_{1-x}Ni_xO_3$ ($0 \le x \le 0.5$) samples.[16] The $LaFe_{1-x}Ni_xO_3$ ($x = 0.3$, 0.4 & 0.5) thin films grown on $LaAlO_3$ (LAO) substrates by pulsed laser deposition also demonstrated the FM and semiconducting property.[17]

†Corresponding author. E-mail: famirnit@gmail.com

© 2014 Chinese Physical Society and IOP Publishing Ltd

Even when these films of $LaFe_{1-x}Ni_xO_3$ ($x = 0.3$, 0.4 & 0.5) were irradiated by heavy ions they showed the same semiconducting and ferromagnetic FM behaviors with some modifications.[18,19]

In the present paper, we attempt to observe the effects of Ni doping on DC magnetization and magneto-transport properties of $PrFe_{1-x}Ni_xO_3$ ($x = 0.1$, 0.2, 0.3, 0.4, and 0.5) thin films prepared by pulsed laser ablation deposited on $LaAlO_3$ (001) orientated substrates.

2. Experiments

The bulk samples (as film target) of $PrFe_{1-x}Ni_xO_3$ ($x = 0$, 0.1, 0.2, 0.3, 0.4, and 0.5) were prepared by a ceramic reaction technique.[16] Thin films of $PrFe_{1-x}Ni_xO_3$ ($x = 0$, 0.1, 0.2, 0.3, 0.4, and 0.5) were deposited on single-crystal substrates of (001) orientated $LaAlO_3$ by pulsed laser ablation technique. The grown films each have a thickness of around 200 nm but the film with composition $x = 0.3$ is thicker than that with the other compositions. The film growth (conditions or growth parameters etc.), structural and electrical characterizations have already been published elsewhere.[20]

The temperature dependences of resistivity ($H = 0$ and $H = 9$ T) and magnetic measurements were investigated using a superconducting quantum interference device magnetometer (Quantum design, PPMS-9).

3. Results and discussion

3.1. DC magnetization study

In order to see the effect of Ni^{3+} ion substitution in $PrFeO_3$ matrix, zero field-cooled (ZFC) and field-cooled (FC) magnetization measurement have been investigated. Figure 1 shows the ZFC and FC dc magnetizations each as a function of temperature for $PrFe_{1-x}Ni_xO_3$ ($0 \leq x \leq 0.4$) thin films. In the ZFC process, the sample is cooled in the zero field from 300 K to 5 K and the magnetization is measured in the presence of a medium magnetic field ($H = 500$ Oe, 1 Oe = 79.5775 A/m), during the warming up cycle. In the FC process, the same field is applied while cooling the sample from 300 K to 5 K and the magnetization measurements are performed during the warming up cycle. It is observed that the magnetization decreases with the increase of temperature.

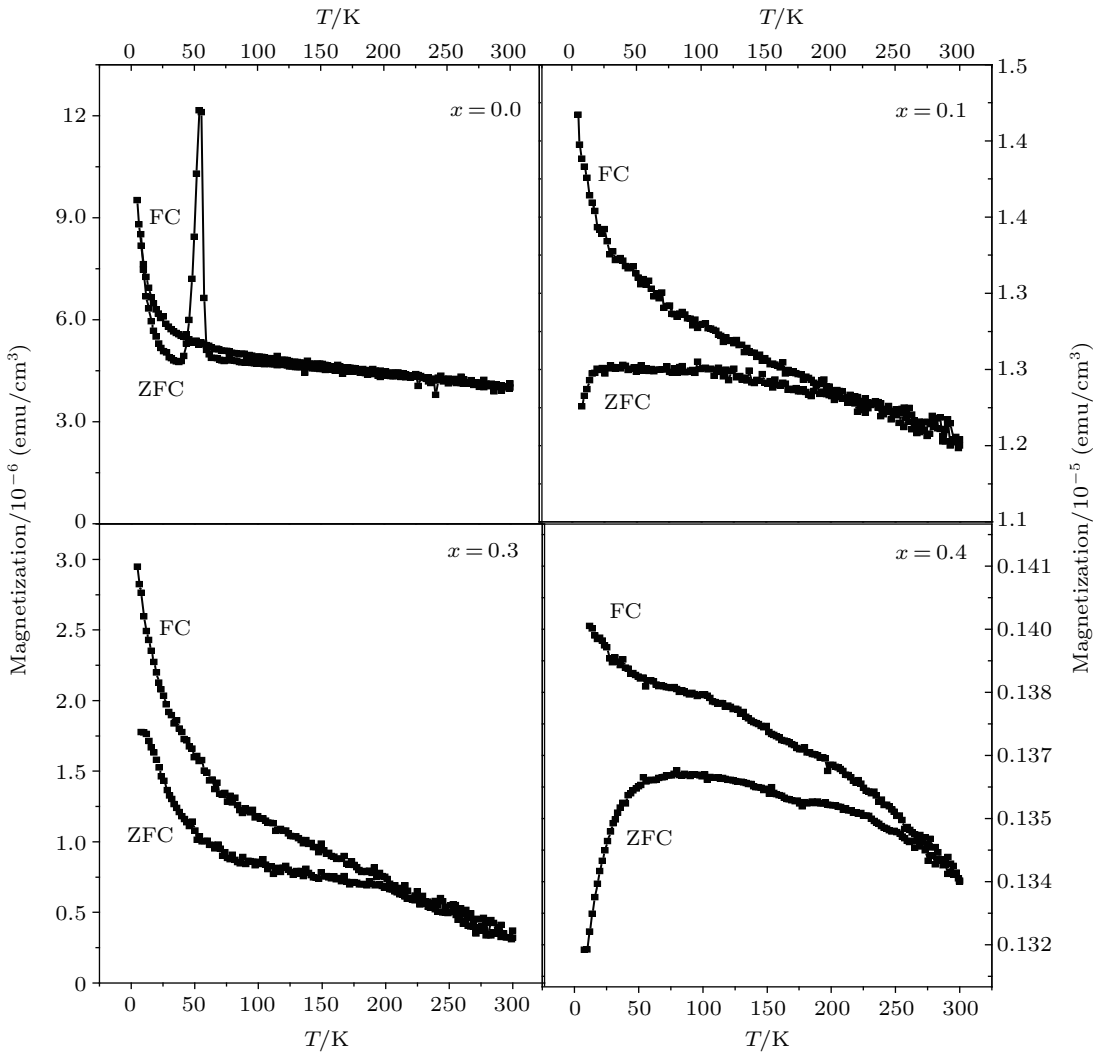


Fig. 1. Temperature dependences of magnetization measured for specimens of $PrFe_{1-x}Ni_xO_3$ ($x = 0.0$, 0.1, 0.3, and 0.4) at temperatures between 5 K and 300 K in an applied field of 500 Oe.

The temperature at which the FC and ZFC curves take part can be used as an indicator of the magnetic ordering temperature. Judging from the weak field-induced magnetization, the overall behavior is AFM, but the magnetic irreversibility and in particular the small FC magnetizations observed at low temperature indicate a weak FM-like behavior. Application of the Goodenough–Kanamori rules to all the possible bifurcation/ordering behavior is expected to arise as a consequence of the different signs of the magnetic interactions among d^5Fe^{3+}, d^4Fe^{4+}, d^7Ni^{3+}, and d^8Ni^{2+} present in the lattice. It has been previously suggested that a spin-glass behavior exists at low temperatures for $LaFe_{1-x}Ni_xO_3$ ($x < 0.8$) appealing to multiplicity of interactions expected among the different magnetic centers found in Ref. [21]. A plot of the inverse susceptibility as a function of temperature (Fig. 2) shows that strong interactions among magnetic centers exist well in the system. The extrapolation of the slope of the curve (the straight line in Fig. 2) always gives a negative intercept (for lower value of doping) with the horizontal axis, which implies that the prevalent interactions are AFM. The bifurcation/ordering temperature is unusually high (265 K–273 K) which evidences the presence of strong local magnetic interactions in the sample, although the long-range magnetic order is weak or absent. The difference between the FC and ZFC curves up to this ordering temperature indicates that the FM moments persist up to transition point. More precisely, the present behavior observed in the system is due to the disorder of Ni^{3+} and Fe^{3+} ions as well as the interactions between their competing ferromagnetism and antiferromagnetism.

In order to better emphasize the singularities of the magnetization curves, we use the differential curve $[\chi_{FC}(T) - \chi_{ZFC}(T)]$ [21,22] (see the inset of Fig. 3). Neel temperature (T_N) in the case of $PrFeO_3$ is high ($T_N \approx 700$ K),[23] but after Ni doping, owing to the substrate-induced strain, it would have gone down and is observed clearly in the present system.

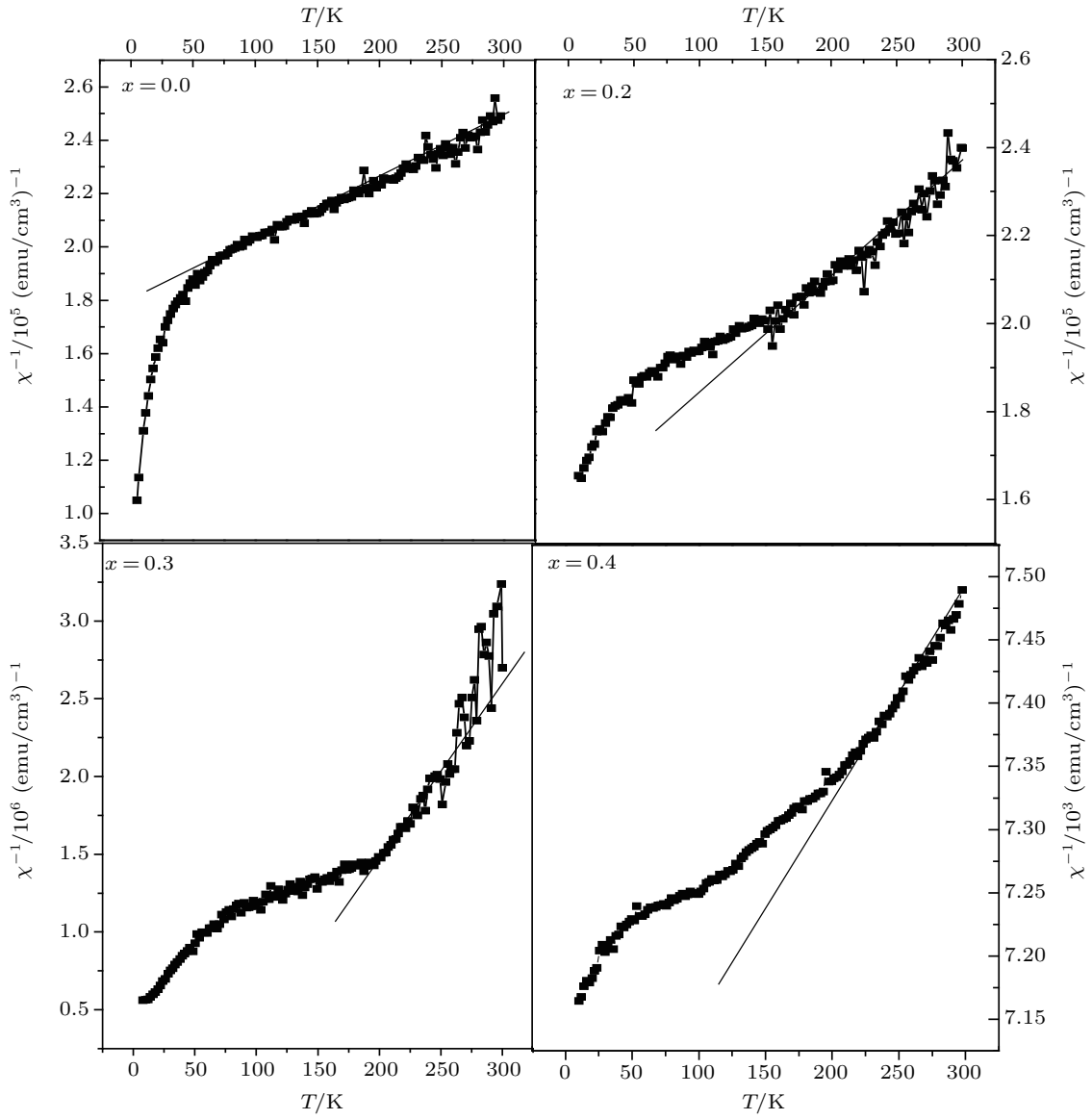


Fig. 2. Temperature dependences of the inverse magnetic susceptibility χ^{-1} for specimens of $PrFe_{1-x}Ni_xO_3$ ($x = 0.0$, 0.2, 0.3, and 0.4).

Again for $x = 0$ composition ($PrFeO_3$) , ZFC shows a sharp peak (see Fig. 1) at about 50 K, which can be attributed to the Hopkinson effect arising from the magnetic anisotropy in the domain structure.[20,24] Recently single crystal of $PrFeO_3$ shows the same trend at about 50 K.[25] This anomaly at 50 K may be considered to be due to the orientation of the Fe^{3+} spins as the family of $RFeO_3$ (R =Nd, Sm, and Er) shows spin reorientation transitions.[25] However to visualize this behavior fully, it needs further study.

Also from Fig. 2, which shows the temperature dependences of the inverse magnetic susceptibility χ^{-1} for $PrFe_{1-x}Ni_xO_3$ thin films ($0 < x < 0.4$). The nonlinear function of reciprocal susceptibility versus temperature in the measured temperature range also confirms the weak FM order. The effective magnetic moment $p_{\rm eff}$ is determined by fitting the Curie–Weiss law to the χ^{-1}–T data

$$\chi = C/T - \theta, \tag{1}$$

where $C = (\mu_0 N_{\rm A}\mu_{\rm B}/3k_{\rm B}) \times p_{\rm eff}^2 =$ Curie constant, $N_{\rm A}$ is the Avogadro's number, $\mu_{\rm B}$ is the Bohr magneton, $p_{\rm eff}$ is the effective magnetic moment, $k_{\rm B}$ is the Boltzmann constant, and θ is the Weiss temperature. $p_{\rm eff}$ decreases as Ni content increases. In general, since the free ion magnetic moment of Fe^{3+} (5.82 $\mu_{\rm B}$) is larger than that of Ni^{3+} (4.82 $\mu_{\rm B}$), the $p_{\rm eff}$ of $PrFe_{1-x}Ni_xO_3$ thin film should decrease with the increase of Ni content. The total effective magnetic moments in $PrFe_{1-x}Ni_xO_3$ are calculated to be 5.91 $\mu_{\rm B}$, 5.84 $\mu_{\rm B}$, 5.51 $\mu_{\rm B}$, 5.03 $\mu_{\rm B}$, 4.71 $\mu_{\rm B}$, and 4.35 $\mu_{\rm B}$ for samples with $x = 0.0$, 0.1, 0.2, 0.3, 0.4, and 0.5, respectively. Because only Fe^{3+} and Ni^{3+} ions contribute to the total effective magnetic moment in $PrFe_{1-x}Ni_xO_3$, the spin state S of Fe^{3+} can be used to calculate $p_{\rm eff}$ via the formula $p_{\rm eff} = [4S(1+S)]^{1/2}$.[26] More precisely, the $\mu_{\rm so} = [(1-x)\mu_{\rm Fe}^2 + x\mu_{\rm Ni}^2]^{1/2}$ is used to do calculations. In the present case, Fe^{3+} ions in $PrFe_{1-x}Ni_xO_3$ have five electrons in the 3d shell, which leads to a total possible spin quantum number S being 1/2, 3/2, and 5/2. Therefore, the possible values of $p_{\rm eff}$ are 5.916 $\mu_{\rm B}/Fe^{3+}$ for the high spin state (HS), 3.873 $\mu_{\rm B}/Fe^{3+}$ for the intermediate spin state, and 1.732 $\mu_{\rm B}/Fe^{3+}$ for the low spin state. Compared with the results from linear fitting of the $1/\chi$–T curves, the spin state (for Fe^{3+} ion) is found to be HS for all the samples. However, the spin state Ni^{3+} ions are assumed to be in low spin state in $PrFe_{1-x}Ni_xO_3$. This is also confirmed from electronic structure study of its bulk (used as film target for the present films) as well as these thin films.[16] It was discussed in the previous report that the bond angle of M–O(2)–M increases with the increase of Ni content.[20] The increase in the bond angle may enhance AFM, super-exchange interaction between Fe^{3+}–Fe^{3+} and Fe^{3+}–Ni^{3+} and contribute to the magnitude of θ (Table 1). Here a decrease in θ may be due to the fall in negative molecular field with the decrease in AFM frustration. In addition, the AFM frustration gives rise to weak FM component which is created from the canted–AFM spin arrangement of Fe^{3+} magnetic moment.[26] In the cases of $RFe_{1-x}Ni_xO_3$ (R = Nd, Sm) bulk system, the values of $p_{\rm eff}$ are different from those of $PrFe_{1-x}Ni_xO_3$ thin films, reflecting the differences in the rare-earth moment and dimensions of the system (thin film),[27] which represents the fall in negative molecular field and consequent decrease in AFM frustration. Also the AFM frustration leads to weak FM component which arises from the canted AFM spin arrangement of Fe^{3+} magnetic moment.

Table 1. Parameters extracted from magnetization hysteresis curves.

x	Coercive field $H_{\rm C}$/Oe	Saturation field ($M_{\rm S}$)	Weiss-temperature θ/K
0.0	18.88	0.00168	−375
0.1	102.43	0.00051	−250
0.2	50.7	0.0001	−25
0.3	52.35	0.00178	75
0.4	46.76	0.00108	100
0.5	33.68	0.00090	–

In Fig. 3, we show magnetic hysteresis loops at room temperature for all the samples. A small hysteresis loop with good coercivity is seen in each case (see Table 1). The saturation magnetization decreases with the increase in the Ni concentration (but not systematically). The different coercive fields in a series of members of FM semiconductors having different saturation magnetizations are not new.[28] However, it should be pointed out here that coercivity of a magnetic thin film depends on various factors, such as micromagnetic structure of the film, magnetic anisotropy constant, magnetic exchange energy, saturation magnetization, inter grain domain wall, grain size, micro-structural defects, etc. To estimate the contribution from each of these factors is beyond the scope of the present work. However, an effort is made to discuss a few of them below.

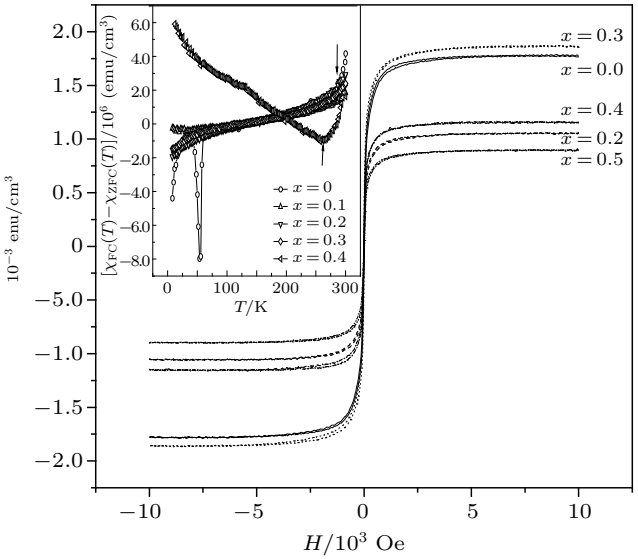


Fig. 3. Isothermal magnetization hysteresis of $PrFe_{1-x}Ni_xO_3$ ($x = 0.0$, 0.2, 0.3, 0.4, and 0.5) at 300 K. The inset shows differential curves $[\chi_{\rm FC}(T) - \chi_{\rm ZFC}(T)]$ for $x = 0.0$, 0.2, 0.3, 0.4 compositions and arrows show their values of $T_{\rm N}$.

It can be seen from Fig. 4 that for $PrFe_{1-x}Ni_xO_3$ (for $x = 0.1$, 0.2, 0.33, and 0.5) thin films with nearly the same particle size, M_S has a tendency to decrease with the increase of Ni content. There are many factors such as the crystal structure, Ni^{3+} content, and the formation of Fe^{4+} (or Ni^{2+}) ions that may influence the weak ferromagnetism in the prepared film. Although the interparticle interaction may have an influence on the magnetic behavior of the magnetic particle system, as the moment of the magnetic particle is very small in the prepared sample, the effect of interparticle interaction is probably negligible in this system.

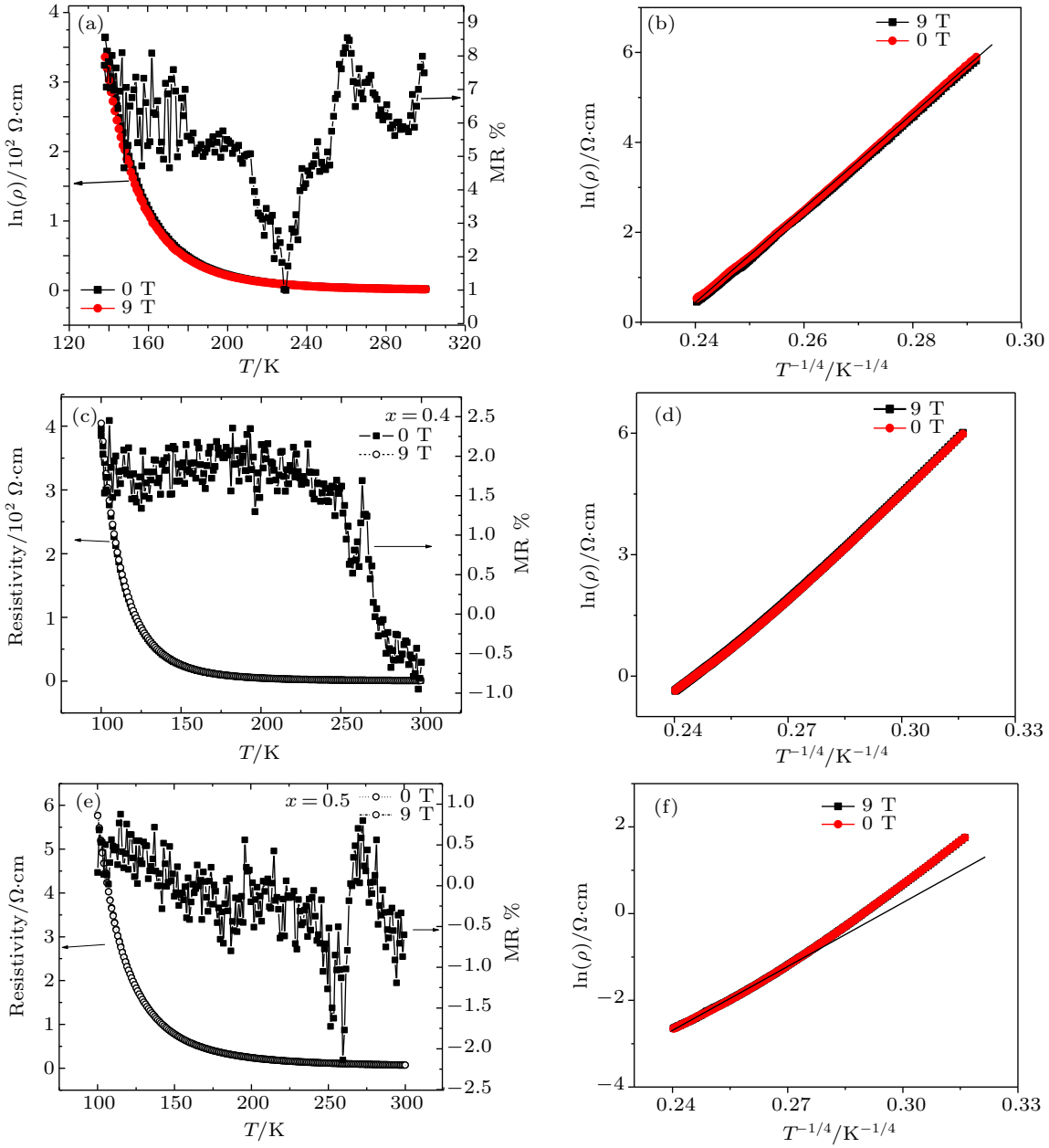


Fig. 4. (color online) (a), (c), and (e) Temperature-dependent resistivity values of the films with $x = 0.3$, $x = 0.4$, and $x = 0.5$ composition under 0 T and 9 T field along with their magnetoresistances respectively, and (b), (d), and (f) their respective VRH fittings.

The magnetic properties are related to the bond overlap between the oxygen p orbital and iron d orbital and the deviation of the Fe–O–Fe angle from 180°. From the above structural analysis, the substitution of Fe^{3+} by Ni^{3+} ions in the $PrFe_{1-x}Ni_xO_3$ thin film causes the decrease in the Fe–O bond length and the increase in the Fe^{3+}–O–Fe^{3+}/Ni^{3+}–O–Ni^{3+}/Fe^{3+}–O–Ni^{3+} bond angle. These two aspects both strengthen the AFM, super-exchange interaction and weaken the existing weak ferromagnetism. Also already discussed, the substitution of Fe^{3+} by Ni^{3+} ions in the $PrFe_{1-x}Ni_xO_3$ thin films may possibly induce different interactions, super-exchange coupling between neighboring pairs of Fe^{3+}–O–Fe^{3+}, Ni^{3+}–O–Ni^{3+} ions and the AFM coupling between Fe^{3+}–O–Ni^{3+} ions. Also the super-exchange interaction could also be AFM between certain valence states and spin states of the Ni ion. The increasing Ni content may lead to the reduction of Fe^{3+} ions and cause the reduction in magnetization. This is because Fe^{3+} is in high spin state and its high spin is a magnet-

ically stable ion. Furthermore, the effective magnetic moment of Fe^{3+} (high spin) is more than that of Ni^{3+} (low spin state). Therefore, it may be concluded that the Fe–O bond length and the Fe–O–Fe bond angle are two important structural parameters that affect the weak ferromagnetism in the $PrFe_{1-x}Ni_xO_3$ thin films. The influence of Ni doping on PrFeO3 thin films has already been discussed in our previous effort.[20]

Furthermore the effect of Ni doping in $PrFe_{1-x}Ni_xO_3$ thin films may lead to different particle sizes, so the saturation magnetization increases/decreases with the decreasing /increasing average particle size. Alternatively, it may be due to the surface effect, finite size effect, and lattice distortion in the $PrFe_{1-x}Ni_xO_3$ thin films. In FM and AFM oxides, magnetic coupling is very sensitive to the atomic environment. When the particle size decreases to less than 100 nm, a large fraction of their atoms are situated on the surface layer where their local orders differ considerably from those of the interior atoms. The atomic disorder and reduced coordination of the surface atoms affect the magnetic interactions, which may lead to a random canting of the surface spins. The existence of non-collinear spin structures on the particle surface has already been demonstrated by Mossbauer spectroscopy in the magnetic nanoparticles such as $CoFe_2O_4$, $NiFe_2O_4$, and $\gamma-Fe_2O_3$ in which non-collinear spin structures progressively diminish with increasing particle sizes.[29–31] Here it should be noted for single domain regions, the saturation magnetization increases whereas in the case of multi-domain it decreases after attaining a constant value.[32] In the multi-domain region the variation of coercivity with particle size can be expressed as[32]

$$H_c = a + b/D, \tag{2}$$

where a and b are constants and D is the particle size. Therefore, in the multi-domain region, the coercivity decreases with particle size reduction. In present films, we have already observed the particle size decreases with Ni substitution [confirmed by x-ray diffraction (XRD) data and atomic force microscopy analysis].[20] This could be one of the reasons for the reduction in saturation magnetization as well as coercivity in our case.

The nanoparticles may be imaged to have a core with the usual spin arrangement and a surface layer in which the spins of the ions are not oriented at random, but are inclined at some angle to their normal direction, and mainly depending on their magnetic nearest neighbors. For the $PrFe_{1-x}Ni_xO_3$ thin films, as the particle size increases, the spin canting at the surface may benefit the reduction of the net FM moment in this canted spin system. The greater the particle size, the lowers the fraction of surface atoms, and the smaller the contribution to the total FM moment. On the other hand, AFM particles are expected to have a net magnetic moment due to uncompensated spins.[33,34]

Finally, the lattice distortion with the change of the particle size in the $PrFe_{1-x}Ni_xO_3$ thin films may provide a clue to understanding the change in the magnetization. From the structure analysis, as the particle size decreases, the Fe–O bond length increases and the Fe–O–Fe bond angle decreases and hence both decrease the degree of overlap between the oxygen and iron. These enhance the AFM interaction and weaken the total FM component. Also the structural distortion occurs because at the external surfaces spins are in a disordered state and have very low coordination of cations due to broken exchange bond which affects the super-exchange interactions.[35,36]

3.2. Magneto resistance (MR)

The plots of electrical resistivity (with $H = 0$ T and $H = 9$ T) versus temperature for the samples ($x = 0.3$, 0.4 & 0.5) are shown in Figs. 4(a), 4(c), and 4(e). All the samples show semiconducting behaviors in the measured temperature range. It is clear from the figures that the resistivity at room temperature is reducing with Ni doping increasing. These resistivity values are considerably smaller than their bulk values.[16] These lower values of resistivity in these thin films may be due to the smaller grain boundary densities than those in bulks, which is also observed in the case of small value of full width at half maximum (FWHM).[20] Generally, at higher temperatures, owing to thermal energy, the carriers are activated to extend states with maximum mobility. To study the electrical conduction mechanism of $PrFe_{1-x}Ni_xO_3$ ($0.3 \leq x \leq 0.5$) thin films, $\rho(T)$ is compared with

$$\rho = \rho_0 \exp(E_a/k_B T), \tag{3}$$

which shows normal thermally activated electrical conductivity[37–39] where an electron or hole (as the charge carrier) moves from one localized state to another due to the interaction between the charge carriers and phonons. In Eq. (3) ρ_0 is the electrical resistivity at high temperatures, E_a is the thermal activation energy (or simple activation energy) of the electron or hole, and k_B is the Boltzmann constant. The electrical resistivity values of $PrFe_{1-x}Ni_xO_3$ ($0.3 \leq x \leq 0.5$) are plotted as $\ln \rho$ versus $1/T$ in (its relevant figure is not shown here), since the data do not show a linear fit in the entire studied temperature range. This indicates that equation (3) cannot be fully implemented. But the above equation can give a rough idea of thermal activation energies in the limited temperature range, where the data can show the best fit.

It should be noted here that the Ni doping in the $PrFeO_3$ gives rise to carrier doping, leads to the decrease in energy gap and hence the increase in electrical conductivity of the compound. Generally, the chemical substitution for the generation of charge carriers brings disorder in the system, which may lead to delocalizing the carriers at the doping site. The carriers in the localized states proceed by a phenomenon known as variable-range-hopping (VRH).[37–39] So in order to understand the effect of disorder-induced localization on the electrical transport properties in the present system we fit our data with Mott's variable range hopping (VRH).[38,39]

According to the Mott's variable-range-hopping (VRH), the expression for electrical resistivity in a three-dimensional system is given by[38]

$$\rho = \rho_0 \exp(T_0/T)^{1/4}, \tag{4}$$

where T_0 is the Mott's characteristic temperature which is related to the density of states at Fermi level $N(E_f)$ and localization length (α) as shown below

$$T_0 = 18\alpha^3/N(E)k_B. \tag{5}$$

It has been observed that the data fit by VRH model to a limited range of temperature (see Figs. 4(b)–4(e)). This is quite consistent with the reported results of a similar system and thus suggests that the conduction is governed by the disorder-induced localization of charge carriers.[38,39]

At room temperature (300 K), we obtain different parameters for DC conductivity by fitting data with the above equations and the results are summarized in Table 2, where the values of T_0 are fit by using $\alpha = 2.5$ Å.[40] The density of states $N(E_f)$ at Fermi level is calculated from the slope of ln(conductivity $xT^{1/2}$) versus $T^{1/4}$. The $N(E_f)$ at Fermi level increases with the increase of content of Ni substitution (see Table 2) and higher values with high concentration are also supported by Refs. [16] and [18]. This may be a possible reason for the increase of conductivity in the present system. The activation energy (E_a) is found to decrease with the increase of Ni concentration as shown in Table 2. With the addition of Ni, the e_g electrons of Fe^{3+} ions become delocalized. It may be possible that the electronic property in the present system is due to the induced distortion effect because of the presence of two different homovalent transition metals (Fe and Ni). As Fe^{3+} (high spin) with $r(Fe^{3+}) = 0.64$ Å is replaced by Ni^{3+} (low spin) with $r(Ni^{3+}) = 0.56$ Å,[34] the Fe–O–Fe or Ni-O–Fe bond angle and its super-exchange angle are changed, which affects the tolerance factor $t = d_{RE\text{-}O}/\sqrt{2(d_{M\text{-}O})}$ and hence influences the transport properties.[20] As it has been established that the transport properties are closely related to the structural distortion and in particular to the arrangement of FeO_6 octahedra,[20] the single particle band width of the system is changed.

Table 2. Physical parameters of $PrFe_{1-x}Ni_xO_3$ ($x = 0.3$, 0.4, and 0.5) thin films, obtained from DC conductivity data with and without applying magnetic field.

	$H = 0$ T			$H = 9$ T		
Samples	$T_0/10^7$ K	W/meV	$N(E_f)/10^{19}$ eV^{-1}·cm^{-3}	$T_0/10^7$ K	W/meV	$N(E_f)/10^{19}$ eV^{-1}·cm^{-3}
$x = 0.3$	16.295	121.35	2.002	17.012	123.22	2.312
$x = 0.4$	11.131	111.9	2.931	12.101	114.01	3.124
$x = 0.5$	3.446	55.55	9.482	3.754	58.12	9.752

Again here figures 4(a)–4(d) show the curves of resistivity versus temperature for $PrFe_{1-x}Ni_xO_3$ ($0.3 \le x \le 0.5$) samples under the magnetic fields in a range of 0 and 9 T. The two curves are almost identical and no changes are observed in the shape and in the absolute value. Such a behavior suggests that no FM polarons are formed in $PrFe_{1-x}Ni_xO_3$ ($0.3 \le x \le 0.5$) contrary to those found in doped Nickelates.[41] The magnetoresistances of these samples show scattered data, hence indicating less interaction between charge carriers or simply the system being least affected by applying high magnetic field (insulating regime). In the insulating regime, the magnetoresistance is low but negative, similar to what is seen in other transition metal oxides.[42] Such a behavior may arise from weak-localization effect.[43] Note here that the charge concentration is small and the system is insulating at all temperatures. Also in the presence of 9-T field, we calculated various fitted parameters [like E_a, T_0, and $N(E_f)$] and present them in Table 2. Since there are not many changes in resistivity in the presence of field, no significant change is observed in these obtained parameters.

As already mentioned above for all the samples, the resistivity values at all the measured temperatures are not sensitive (or are less sensitive) to the applied field. In order to see it more clearly, we plot the curves of magnetoresistance versus temperature (MR $\sim T$) in Figs. 4(a)–4(d). Here the MR is defined as

$$[\Delta\rho/\rho]x\% = [\rho(H=0) - \rho(H)/\rho(H=0)]x100, \tag{6}$$

where $\rho(H = 0)$ is the resistivity in the absence of field and $\rho(H)$ is the resistivity in an applied field of $H = 9$ T.

For the sample $x = 0.3$ the MR is positive and shows decreasing trend but starts to rise at 230 K and again shows decreasing trend at 260 K. For the samples $x = 0.4$ and 0.5, the MR values increase (also their signs change from negative to positive) with cooling down rather slowly, however at about 262 K they sharply increase and then further increase at this rate with further cooling down. These results suggest that the transport properties are completely different from those of the samples $x > 0.3$. This further supports our argument regarding different transport mechanisms in this system.[20] Also according to Ogale *et al.*,[28] the observed GMR effect occurs due to the peculiar electrical transport mechanism in a magnetic disorder state and is directly related to the structural transition. However, we observe irreversibilities or magnetic disorders/disorderings in the M–T curves in our samples. The magnetization data of films with $x = 0.3$, $x = 0.4$, and $x = 0.5$ show a bifurcation trend in ZFC and FC at about the same temperature (260 K), thereby indicating some sorts of disorderings in the present system.

For observing positive MR values at low temperatures, one of the possibilities would be a giant spin splitting of band states caused by the sp–d exchange interaction under applied H due to a Zeeman splitting effect in the vicinity of E_F.[29] This results in the enhancement of electron scattering and thus leads to the sharp increase of resistivity at low temperatures. This spin splitting model seems to be more appropriate to our system as it provides quite a good explanation of data recently reported by Haneda and Morrish,[30] who showed large positive MR $\sim 48\%$ at 10 K in Co, Mn-doped ZnO thin films. Alternatively, low temperature MR enhancement seems to be related to the existence of FM component within the antiferromagnetically ordered state. Further positive value of MR in the system is quite surprising. Although the present oxides cannot qualify for the practical application as such with the present least value of MR, theoretical implications may be interesting. More precisely, deeper investigations of the magnetic properties of this composite system are essential to clarify this situation.

4. Conclusion

In this paper, we have successfully synthesized the epitaxial thin films of $PrFe_{1-x}Ni_xO_3$ ($x = 0$, 0.1, 0.2 ,0.3, 0.4, and 0.5) by PLD technique on LAO substrates. The effect of Ni ion doping on magnetic properties of $PrFeO_3$ is studied. The DC magnetization hysteresis loop study reveals weak ferromagnetic/ferrimagnetic nature, saturation magnetization increases/decreases with the content of Ni substitution. The zero field cooled (ZFC) and field cooled (FC) magnetization study infers that the magnetic frustration exists with Ni doping. It is concluded that the Fe–O bond length and the Fe–O–Fe bond angle are two important structural parameters that affect the weak ferromagnetism in the $PrFe_{1-x}Ni_xO_3$ thin films. Resistance values in the presence of magnetic field for some samples ($x = 0.3$, 0.4, and 0.5) show the least effect. Various essential parameters, electric conductivity like E_a, T_0, and $N(E_f)$ are calculated in the absence and in the presence of field. Some factors are explored to explain the present data.

Acknowledgment

The authors would like to thank Director and Dr. R. J. Choudary, IUC-CSR Indore (M. P) India for some experimental facilities and fruitful discussion and also thank Dr. M. Ikram (NIT Srinagar) for his encouragement and moral support.

References

[1] Rao C N R and Raveau B 1998 *Transition Metal Oxides: Structure, Properties, and Synthesis of Ceramic Oxides*, 2nd edn. (New York: Wiley-VCH).
[2] Cornell R M and Schwertmann U 2003 *The Iron Oxides: Structure, Properties, Reactions, Occurrences, and Uses*, 2nd edn. (Weinheim: Wiley-VCH)
[3] Wang X, Yang G Z and Lu H B 2008 *Chin. Phys. Lett.* **25** 663
[4] Chen Z H, Sun W G and Wu W D 2008 *Chin. Phys. Lett.* **25** 1465
[5] Wang W T, Yang G and Duan P 2002 *Chin. Phys. Lett.* **19** 1122
[6] Wang L W, Gao J X and Huang B P 1998 *Chin. Phys. Lett.* **15** 764
[7] Yang G Z, Lü H B, Wang H S, Cui D F, Yang H Q, Wang H, Zhou Y L and Chen Z H 1997 *Chin. Phys. Lett.* **14** 478
[8] Ueda K, Tabata H and Kawai T 1999 *Jpn. J. Appl. Phys.* **38** 6690
[9] Burns R G 1981 *Perovskite: A Structure of Great Interest to Geophysics and Materials Science*, ed. Navrotsky A and Weidner D J (Washington: Am. Geophys. Union) p. 81
[10] Park J H, Kimura T and Tokura Y 1998 *Phys. Rev. B* **58** 13330
[11] Wu Z Y, Benfatto M, Pedio M, Cimino R, Mobilio S, Barman S R, Maiti K and Sarma D D 1997 *Phys. Rev. B* **56** 2228
[12] Eibschutz M, Shtrikman S and Treves D 1967 *Phys. Rev.* **156** 562
[13] Treves D 1965 *J. Appl. Phys.* **36** 1033
[14] Dai H, He H, Li P, Gao L and Au C 2004 *Catal. Today* **90** 231
[15] Marezio M and Dernier P D 1971 *Mater. Res. Bull.* **6** 230
[16] Kumar R, Choudhary R J, Ikram M, Shukla D K, Mollah S, Thakur P, Chae K H, Angadi B and Choi W K 2007 *J. Appl. Phys.* **102** 033703
[17] Choudhary R J, Kumar R, Srivastava J P, Patil S I, Arora S K and Shvets I V 2005 *Appl. Phys. Lett.* **87** 132104
[18] Khan M W, Khan M A M, Alhoshan M, AlSalhi M S, Aldwayyan A S, Kumar R and Shahid H 2010 *J. Appl. Phys.* **107** 093704
[19] Choudhary R J, Kumar R, Khan M W, Srivastava J P, Patil S I, Arora S K and Shvets I V 2008 *Nucl. Instrm. Methods Phys. Res. B* **266** 1611
[20] Feroz Ahmad, Mir M Ikram and Ravi kumar 2012 *Phil. Mag.* **92** 1058
[21] Goodenough J B 1996 *J. Solid State Chem.* **127** 126
[22] Bombik A, Leśniewska B and Pacyna A W 2002 *J. Magn. Magn. Mater.* **241** 25
[23] Bombik A, Pacyna A W and Witek W 1994 *Acta Phys. Pol. A* **85** 263
[24] Demazeau G, Marbeuf A, Pouchard M and Hagenmuller P 1971 *J. Solid State Chem.* **3** 582
[25] Wang X Y, Cao S X, Wang Y B, Yuan S J, Kang B J, Wu A H and Zhang J C 2013 *J. Crystal Growth* **362** 216
[26] Andrzej, Barbara, Jacek M and Andrzej P 2003 *J. Magn. Magn. Mater.* **257** 206
[27] Nagata Y 2001 *J. Magn. Magn. Mater.* **237** 250
[28] Ogale S B, Choudhary R J, Buban J P, Lofland S E, Shinde S R, Kale S N, Kulkarni V N, Higgins J, Lanci C, Simpson J R, Browning N D, Das Sarma S, Drew H D, Greene R L and Venkatesan T 2003 *Phys. Rev. Lett.* **91** 077205
[29] Slawaka-Waniewska A, Didukh P, Greneche J M and Fannin P C 2000 *J. Magn. Magn. Mater.* **227** 215
[30] Haneda K and Morrish A H 1988 *J. Appl. Phys.* **63** 4258
[31] Morrish A H and Haneda K 1981 *J. Appl. Phys.* **52** 2496
[32] Cullity B D 2009 *Introduction to Magnetic Materials* (New Jersey: Wiley)
[33] Zysler R, Fiorani D, Dormann J L and Testa A M 1994 *J. Magn. Magn. Mater.* **133** 71
[34] Richardson J T, Yiagas D I, Turk B, Forster K and Twigg M V 1991 *J. Appl. Phys.* **70** 6977
[35] Kodama R H, Berkowitz A E, McNiff E J and Foner S 1996 *Phys. Rev. Lett.* **77** 394
[36] Jiles D C 1997 *Introduction to Magnetism and Magnetic Materials*, 2nd edn. (London: Taylor and Francis)
[37] Mott N F 1968 *J. Non-Cryst. Solids* **1** 1
[38] Austin I G and Mott N F 1969 *Adv. Phys.* **18** 41
[39] Mott N F and Davis E A 1979 *Electronic Processes in Non-Crystalline Materials*, 2nd edn. (Oxford: Clarendon)
[40] Sonia B A, Nabil K, Sami K, Thierry G, Octavio P and Mohamed O 2013 *J. Supercond. Nov. Magn.* **26** 3171
[41] Blasco J and Garc?a J 1994 *Solid State Commun.* **91** 381
[42] Raychaudhuri A K 1995 *Adv. Phys.* **44** 21
[43] Blasco J and Garcıa J 1994 *J. Phys.: Condens. Matter* **6** 5875
[44] Zhang L, Huang B, Liu Y, Zhang L, Zhang R and Mei L 2003 *J. Magn. Magn. Mater.* **261** 257
[45] Sawicki M, Dietl T, Kossut J, Igalson J, Wojtowicz T and Plesiewicz W 1986 *Phys. Rev. Lett.* **56** 508
[46] Wang J, Gu Z, Lu M, Wu D, Yuan C, Zhang S, Chen Y, Zhu S and Zhu Y 2006 *Appl. Phys. Lett.* **88** 252110